Development of Sacrificial Zn-Sn Coatings by Pulse Electrodeposition Process

Yoon-Seok Choi, Prabhu Ganesan, Swaminatha P. Kumaraguru and Branko N. Popov
Department of Chemical Engineering, University of South Carolina, Columbia, SC 29208, USA

Zn-Sn deposits with the Zn content varying from 85 to 22 wt. % were pulse electroplated onto steel substrate from an acid sulphate plating bath. The corrosion behavior of Zn-Sn deposits including sacrificial property were determined in 5% NaCl solution by open-circuit potential measurement, potentiodynamic test, and electrochemical impedance spectroscopy (EIS). The open-circuit potential of Zn-Sn deposits are similar to that of a pure Zn, regardless the Zn amount in the deposit. This indicates that the initial corrosion behavior of Zn-Sn coating system is determined by the sacrificial properties of Zn due to the phase separation of Zn and Sn in the deposit.

For more information
Prof. Branko N. Popov
301 Main Street, Columbia
SC 29208, USA
Phone: 1 (803) 777 7314
Fax: 1 (803) 777 8265
E-mail: Popov@engr.sc.edu

Introduction

Growing ecological concerns in recent years have led to a search for an alternative coating that can effectively replace cadmium coatings. The most commonly used sacrificial coating in place of cadmium is zinc and its alloys. Zinc due to its low standard electrode potential, makes it suitable to act as a sacrificial coating on steel[1]. Several Zn alloy coatings such as Zn-Ni, Zn-Co, Zn-Fe and Sn-Zn provide good corrosion protection to steel.[2-5]. Among them, Zn-Sn holds more potential as a substitute for cadmium in automotive and aerospace industry[6]. It is well known that zinc coatings when exposed to corrosive environments start to dissolve, leading to the formation of basic salts. Tin coatings are quite porous and since tin is cathodic with respect to the steel substrate, the efficiency of corrosion protection depends on the porosity of the coating[7]. Zn-Sn coatings combine the advantages of both metals. In other words, Zn-Sn coatings offer outstanding corrosion protection for steel by combining the barrier protection of tin with the galvanic protection of zinc, without the bulky corrosion product associated with wholly zinc deposits.

Pulse plating (PC), with several plating variables and a higher peak current density compared to DC plating, has received considerable interest in the past 20 years and has proven to be a viable route for material processing[8]. Compared to DC electrodeposition, the pulse plating can improve the deposition process and some deposit properties such as: porosity, ductility, hardness, and surface roughness[9]. For codeposition, pulse plating can produce compositions and structures not obtainable with DC plating[10]. It is expected that pulse plating also may produce Zn-Sn electrodeposits with improved corrosion properties.

There are several compositions which are suggested to offer the best corrosion resistance and protective effect. Traditionally, Zn-Sn coatings with Zn content up to 25 wt.% are widely studied due to the higher corrosion resistance[11]. Previous investigations showed that such coatings are better than or equal to cadmium coatings in salt spray tests and humid atmospheric tests[12]. Based on these investigation results, mainly high Sn content Zn-Sn alloys have been studied. However, from an economic point of view, it is worth developing Zn-Sn deposits with less Sn content.

The aim of this work was to develop PC-deposited Zn-Sn with Sn content less than 25 wt.%, to ensure that the coating will exhibit sacrificial properties while providing extended life in corroding media. The corrosion characteristics of these Zn-Sn deposits have been compared to that of DC-deposited Zn-Sn.

Experimental procedure

Materials

Plating and subsequent corrosion studies were done on low carbon cold-rolled steel plate with thickness of 0.8 mm. Initially, the steel sample was mechanically polished with successively finer grades of emery paper. The samples were then degreased with methanol and rinsed with deionized water.

Before plating, the samples were treated in 10% (v/v) H_2SO_4 solution for 1 min to remove any adherent oxide layer present on the surface, and then washed in deionized water.

Pulse electroplating

Zn-Sn coatings were prepared from a bath containing 110 g/L $ZnSO_4 \cdot 7H_2O$, 5 g/L $SnSO_4$, 80 g/L NH_4Cl, 20 g/L Na-gluconate, 30 g/L Na-citrate at room temperature, and the pH values were varied from 3.7 (as-received) to 7.7 (adjusted using NH_4OH solution). All solutions were prepared with analytical grade reagents and triply distilled water.

The electrodeposited size of the sample was 10 cm^2. Platinum mesh was used as an anode. A pulse generator controlled both the pulse wave and the deposition current density. The average current density for the pulse deposition was varied between 8 and 15 mA/cm^2 while keeping the duty cycle (θ=0.1) and duration (30 min) constant to optimize the deposition rate. After plating, the deposits were rinsed immediately in deionized water, dried with hot air, and subject to further characterization and property measurements.

Characterization

The compositions of the coatings were measured using Energy Dispersive Analysis using X-Ray (EDAX) and X-Ray Fluorescence (XRF). To ensure the accuracy, EDAX and XRF analyses were done at several points on the surface of the sample. The accuracy of the measurements for the equipment used was rated as ±0.1-wt%. The surface morphology and the microstructure of the coating were analyzed using Scanning Electron Microscopy (SEM). The thickness of the specimens was measured using cross-sectional SEM and XRF analyses. The phases of deposits were determined from an X-ray diffractometry (XRD) using a Cu target.

Electrochemical characterization

The electrochemical characterization was done using a three-electrode setup. The steel substrate with the coating was used as a working electrode and a graphite rod was used as a counter electrode. A saturated calomel electrode (SCE) was used as a reference electrode.

Cyclic voltammetric (CV) experiments were carried out with different scan rate in the plating bath. Only one cycle was run in each CV measurement, scanning towards negative potentials.

Potentiodynamic polarization test were carried out in 5% NaCl to evaluate the overall corrosion behavior of the Zn-Sn coatings. The specimen was allowed to attain a stable open-circuit potential (OCP) before starting the polarization scan. A period of ~10 min was required for the OCP to become stable within ± 5 mV. After immersion of the working electrode in the solution for 10 min, the potential

of the electrode was swept at a rate of 0.5 mV/sec from the initial potential of -0.25 V vs. OCP to the final potential of 0 V vs. SCE.

Electrochemical impedance spectroscopy (EIS) measurements were performed in 5% NaCl as a function of time. EIS measurements were conducted at OCP with a 5 mV (rms) perturbation and 10 points per decade using frequency response analyzer. The frequency range covered was from 10 kHz to 10 mHz. The experimental results were interpreted on the basis of an equivalent circuit determined using a suitable fitting procedure described in the fitting program.

Results and discussion

Figure 1 shows the cyclic voltammograms of Zn-Sn deposit on carbon steel in plating solution (pH 3.7) with different scan rates. The CV curve represents two reduction peaks in the negative scan. The peak shown at around -0.8 V can be attributed to the Sn reduction, whereas shown at around -1.4 V can be attributed to the Zn reduction. Both peak currents are shifted with varying the square root of the scan rate indicating a diffusion controlled process.[13]

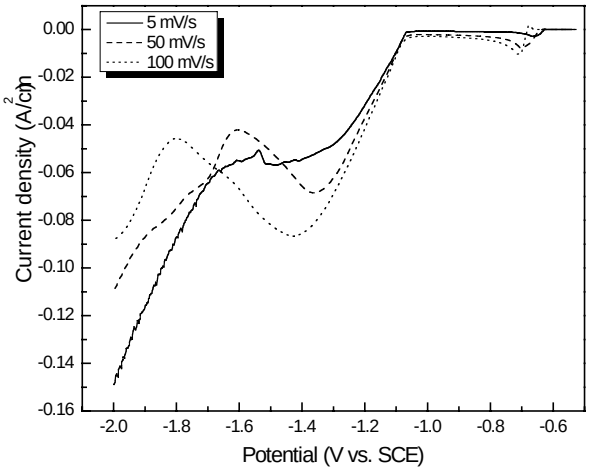

Figure 1: Cyclic voltammograms of steel in Zn-Sn bath with different scan rate.

Figure 2 shows the effect of average current density on the Zn and Sn content in the final deposit. It can be seen that, at lower current densities, as high as 95 wt.% Sn was deposited at room temperature without stirring. The Sn content was reduced to 40 wt.% at 4 mA/cm^2 and gradually decreased with increasing current density. No abrupt variation in the composition was observed above 15 mA/cm^2. In the present study, in order to obtain sacrificial Zn-Sn deposits with Sn content less than 25%, the current densities were selected as 8, 10 and 15 mA/cm^2.

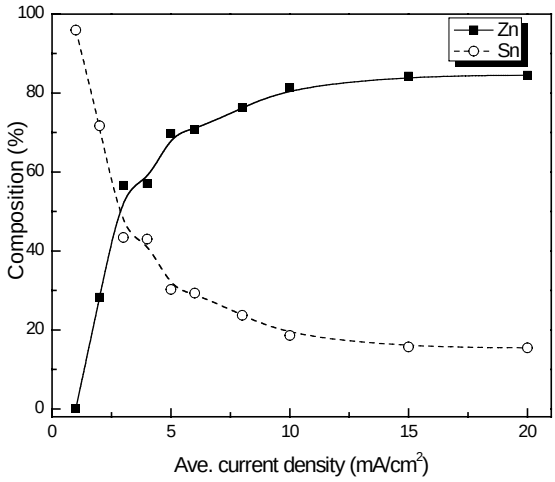

Figure 2: Effect of average current density on the composition of Zn and Sn.

Figure 3 shows the cyclic voltammograms recorded at different pH for the Zn-Sn deposits on carbon steel in plating solution. It can be seen that, at more acidic pH, the Sn^{2+} and Zn^{2+} reduction potentials are more positive and it starts to shift towards more negative potentials with increasing pH. However, it is observed that the potential difference between Zn^{2+} and Sn^{2+} reduction peaks shows smallest value at pH 5.7, indicating a better condition for codeposition of Zn and Sn[14]. The cathodic peak started after Zn deposition may be due to the hydrogen evolution, which decreases as the pH of the bath increase. In addition, in the case of pH 3.7, a new reduction peak can be observed at about -1.7 V. According to Pourbaix diagram of Sn[15], the hydrogen can form metastable phase with Sn as SnH_4 at higher overpotential. The formation of these metallic hydrogenated metastable phases can reduce the current efficiency[16]. In practice, these precipitates can be observed on the surface of deposit after deposition at pH 3.7 for all current densities.

As shown in Fig. 4, the change of the pH of the electrolyte didn't show any effect on the Zn and Sn composition in the deposits. The Zn and Sn contents varied only approximately 3wt % when the same current density but different pH were used to deposit the plates. The current efficiency for the Zn-Sn deposition process increased when the pH of the bath was changed from 3.7 to 7.7 (Figure 5). No variation of the efficiency was observed at pH higher than 5.7. Thus, bath operation was optimized at pH value of 5.7.

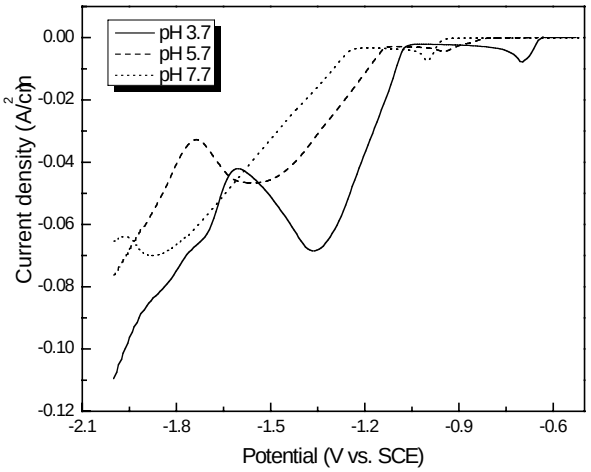

Figure 3: Cyclic voltammograms of steel in Zn-Sn bath with different pH.

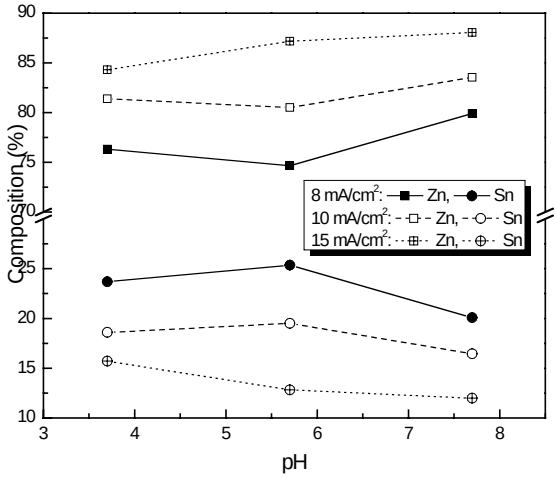

Figure 4: Effect of pH on the composition of Zn and Sn as a function of average current density.

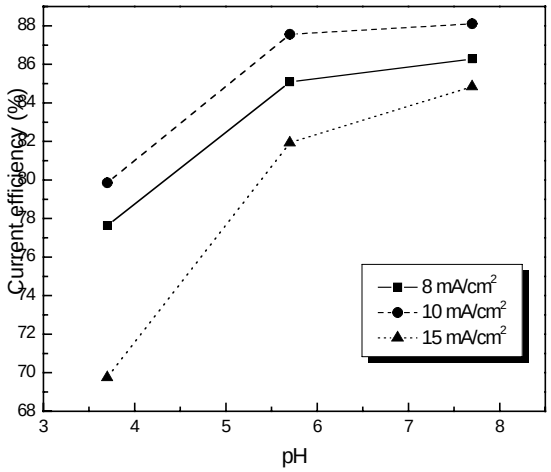

Figure 5: Effect of pH on the current efficiency of the Zn-Sn deposits as a function of average current density.

The compositions of deposits prepared by DC deposition are compared with PC deposition in Figure 6. The deposition was carried out at pH 5.7 with different current densities and deposition methods. In both cases, Zn amount of deposits increase with increasing current density due to the higher rate of Zn deposition. Very small difference of composition is observed between PC and DC deposition processes.

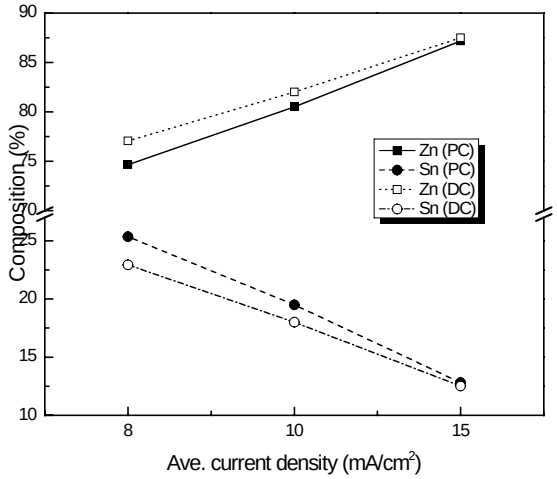

Figure 6: Effect of average current density on the composition of Zn and Sn for PC- and DC-deposited Zn-Sn.

The effect of average current density on surface morphology of PC-deposited Zn-Sn is shown in Figure 7. When the average current density increases from 8 to 15 mA/cm^2, finer grain is obtained in the range of 3 μm, and the distribution of grain size is more homogeneous. Change in the grain size with average current density observed in the present study resulted mainly from variation in the nucleation rate. In the case of PC deposition, metal ions diffuse into the surface of the specimen during the off time so that it is possible for the electrodeposition to be performed at higher peak current density[17]. According to the electrocrystallization theory, a high overpotential usually caused by high current density, speeds up the nucleation process and results in fine grained deposits[18]. However, in the case of DC deposition, similar textured structure was obtained with average current density as shown in Figure 8. At the same average current density, the grain size obtained in PC deposition being smaller than that in DC deposition, and more crystallized structure was obtained by PC deposition. This can be explained by a higher peak current density being used in PC deposition, which increases the nucleation rate.

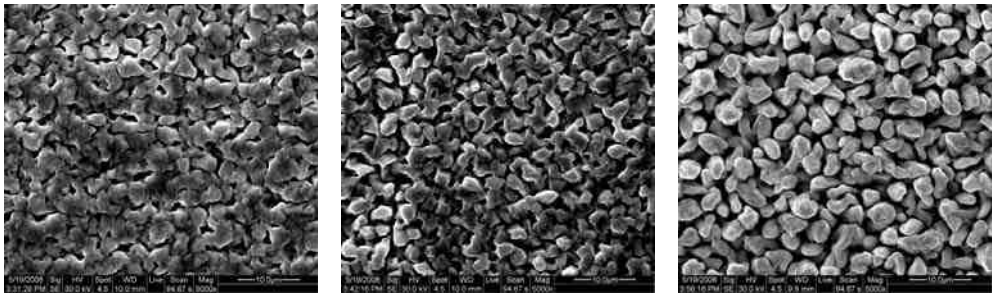

(a) *(b)* *(c)*

Figure 7: SEM micrographs for PC-deposited Zn-Sn with average current density: (a) 8 mA/cm^2, (b) 10 mA/cm^2 and (c) 15 mA/cm^2

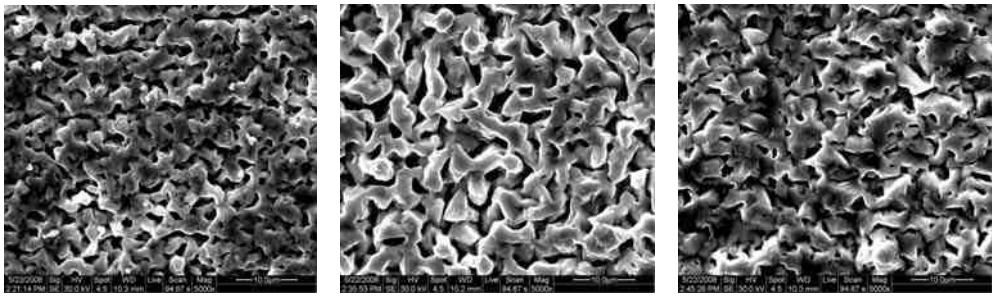

(a) *(b)* *(c)*

Figure 8: SEM micrographs for DC-deposited Zn-Sn with average current density: (a) 8 mA/cm^2, (b) 10 mA/cm^2 and (c) 15 mA/cm^2

Figure 9 shows the XRD patterns of Zn-Sn deposits prepared by DC and PC deposition at 15 mA/cm^2 of average current density. Both deposited coatings represent a mechanical mixture of the zinc phase and tin phase in agreement with literature data[12]. There are several diffraction peaks corresponding to the crystalline faces of Zn and Sn on PC-prepared deposit, indicating that the PC prepared Zn-Sn deposit is composed of polycrystalline Zn and Sn metals. However, some diffraction peaks corresponding to the crystalline faces of Zn disappear in the case of DC prepared Zn-Sn deposit. This suggests that more textured structure is produced by DC deposition, which reduces the crystallization of Zn-Sn deposit.

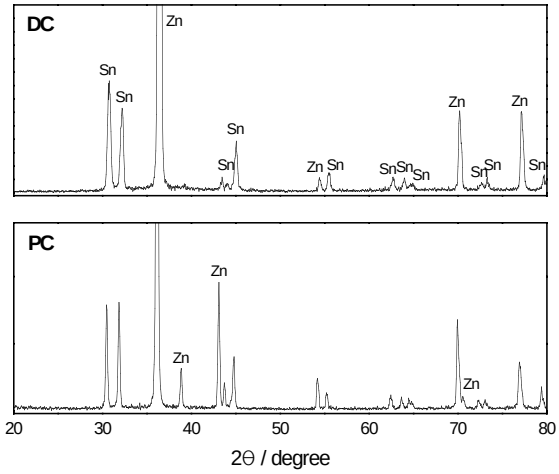

Figure 9: XRD patterns for PC- and DC-deposited Zn-Sn at 15 mA/cm^2 of average current density.

The potentiodynamic polarization curves for PC-deposited Zn-Sn with different average current densities are shown in Figure 10. All coatings exhibited similar corrosion potential between -1.0 ~ -1.2 V vs. SCE. This negative corrosion potential reveals that the corrosion behavior of Zn-Sn deposits is very similar to that of a pure Zn deposit. The pseudo-repassivation region was shown for all samples in the potential range of -0.9 to -0.3 V. This pseudo-repassivation region seemed to be connected with the dissolution of zinc from the coating, which resulted in the formation of a porous, tin-enriched coating through which substrate corrosion initiated. Thus, the current density of this pseudo-repassivation region decreased with increasing the Sn content in the deposit. Figure 11 represents the polarization curves for DC-deposited Zn-Sn with different average current densities. It is similar to the corrosion behavior of PC-deposited Zn-Sn, indicating that the sacrifice of Zn crystal dominates the corrosion behavior.

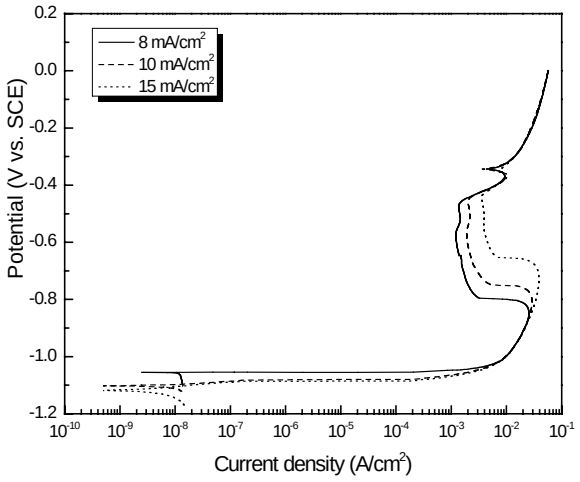

Figure 10: Potentiodynamic polarization curves for PC-deposited Zn-Sn with different average current density in 5% NaCl solution.

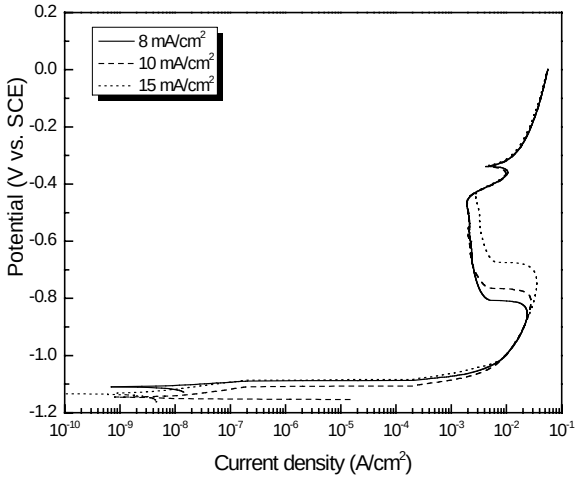

Figure 11: Potentiodynamic polarization curves for DC-deposited Zn-Sn with different average current density in 5% NaCl solution.

Figure 12 shows the corrosion rates of Zn-Sn deposits prepared by DC and PC deposition with different average current densities. In both cases of PC-, and DC-deposited Zn-Sn, the corrosion rate decreased with increasing average current density. In Zn alloy coatings, the corrosion current density increases with the increase in the amount of Zn. The increased corrosion rate in the coatings with

higher amounts of Zn is due to the lowering of the corrosion potential and to an activation of the anodic dissolution of the metal coating due to Zn alloying. However, in the present study, the corrosion rate decreases with increasing Zn content. The decrease in corrosion rate of the Zn-Sn coating with increasing average current density is caused by the formation of galvanic cells between Zn and Sn in the deposit. Unlike other Zn alloy coatings, the Zn-Sn deposits exist as a mechanical mixture consisting of hexagonal close packed Zn phase and tetragonal Sn phase[12]. The presence of Zn and Sn phases as a physical mixture leads to the formation of galvanic couples in the deposit which causes rapid dissolution of Zn from the deposit. The more the amount of Sn present, the higher will be the number of galvanic cell formation and delivering high corrosion rate. From a comparison of the corrosion rate shown in Figure 12, the Zn-Sn prepared by PC deposition at 15 mA/cm^2 exhibits better corrosion resistance than other Zn-Sn deposits. The observed difference in corrosion rate can be explained by taking into account different structure and grain size of the Zn-Sn deposits prepared using DC and PC deposition techniques.

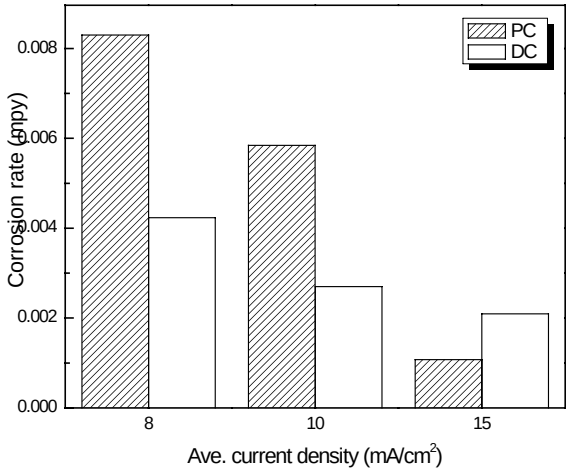

Figure12: Variation of the corrosion rate of Zn-Sn for PC and DC deposits as a function of average current density.

For a better understanding of the effects of structure and grain size on the electrochemical properties of Zn-Sn deposits, EIS measurements were performed. Figures 13 and 14 show Nyquist plots of Zn-Sn deposits prepared by PC and DC depositions at 15 mA/cm^2 of average current density in 5% NaCl solution as a function of immersion time. From an examination of Figures 13 and 14, several interesting features have to be discussed. First, the variation of impedance spectra of PC and DC deposited Zn-Sn shows similar trend with immersion time. Second,

a semicircle arc is generally found in the relative high frequency (HF) range. Third, as the frequency approaches the lower end, a Warburg-like response is found, suggesting that a diffusion process occurs in the low frequency (LF) region.

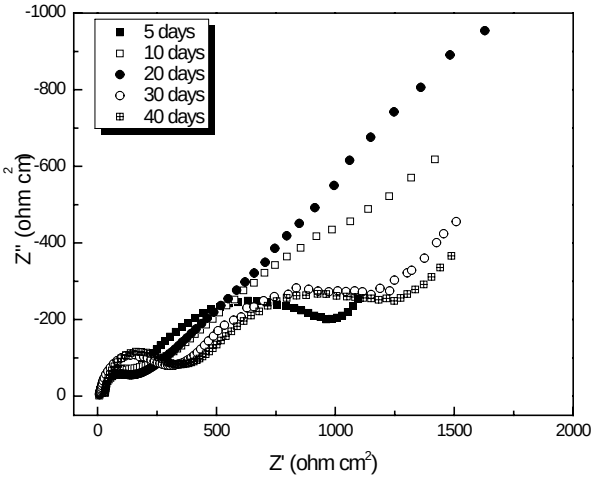

Figure13: Nyquist plots of PC-deposited Zn-Sn as a function of immersion time.

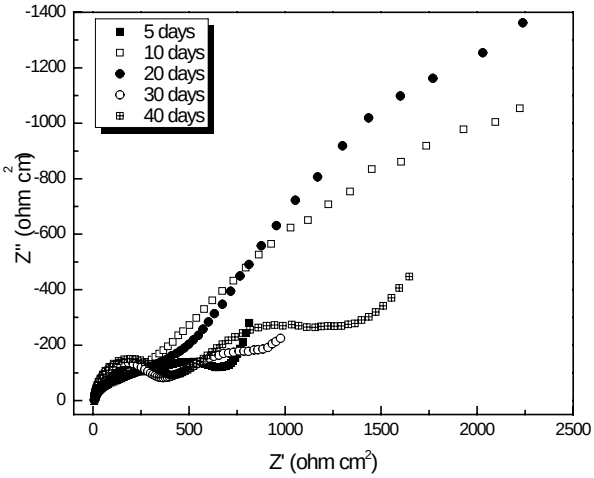

Figure14: Nyquist plots of DC-deposited Zn-Sn as a function of immersion time.

Based on the above results and discussion, an equivalent circuit shown in Figure 15 was applied to model the EIS data. The equivalent circuit consists of the following elements: a solution resistance (R_s) of the test electrolyte between the working electrode and the reference electrode, a capacitance (C_{film}) and a

resistance (R_{film}) for corrosion product of Zn-Sn deposit, and a capacitance (C_{dl}) and a charge transfer resistance (R_{ct}) for Zn-Sn deposit interface. The presence of depressed semi-circles suggests a non-ideal behavior of the capacitors, leading to the introduction of the constant phase element (CPE) in the equivalent circuits. CPE is widely used in data fitting to allow for depressed semicircles[19]. The capacitance is replaced with a CPE for a better fit quality. We do not attempt to measure Warburg impedance coefficient due to the lack of control of the diffusion layer thickness in the stagnant solution. The equivalent circuit was applied to model the EIS data for the individual elements to be determined with a least-squares analysis.

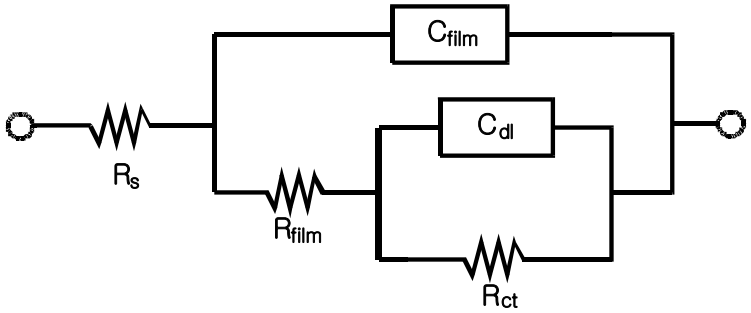

Figure 15: Equivalent circuit to fit the EIS data for Zn-Sn deposits in 5% NaCl solution.

Table 1. Electrochemical parameters obtained by equivalent circuit simulation for PC-deposited Zn-Sn deposits.

Day	R_s (Ω-cm^2)	C_{film} (F/cm^2)	n_1	R_{film} (Ω-cm^2)	C_{dl} (F/cm^2)	n_2	R_{ct} (Ω-cm^2)
5	6.960	9.231×10^{-6}	0.86	148	6.428×10^{-4}	0.55	1033
10	7.018	6.176×10^{-5}	0.65	210.7	1.760×10^{-3}	0.41	4018
20	7.954	1.034×10^{-6}	0.91	76.6	8.837×10^{-4}	0.32	729.7
30	8.963	1.023×10^{-6}	0.86	413.9	4.326×10^{-4}	0.65	791.9
40	9.210	3.362×10^{-7}	0.95	527.8	3.303×10^{-4}	0.69	774.8

Table 2. Electrochemical parameters obtained by equivalent circuit simulation for DC-deposited Zn-Sn deposits.

Day	R_s (Ω-cm^2)	C_{film} (F/cm^2)	n_1	R_{film} (Ω-cm^2)	C_{dl} (F/cm^2)	n_2	R_{ct} (Ω-cm^2)
5	6.174	8.419×10^{-6}	0.88	191.9	7.853×10^{-4}	0.44	709.6
10	6.310	1.748×10^{-5}	0.78	115.3	1.120×10^{-3}	0.39	1443
20	7.412	1.097×10^{-5}	0.80	104.6	4.740×10^{-4}	0.42	448.7
30	7.205	3.904×10^{-7}	0.93	276.5	5.802×10^{-4}	0.39	969.9
40	7.322	3.759×10^{-7}	0.90	573.3	3.040×10^{-4}	0.65	809.7

The optimized values for the various parameters are given in Table 1 and Table 2 for PC- and DC-deposited Zn-Sn, respectively. High values of the CPE power (n_1) and low capacitance (C_{film}) values were influenced by the presence of Zn corrosion products on the sample surface. During immersion time, there is a competition between the continuous renewal of the metal surface and the formation of corrosion products. For small dissolution rates (in particular at open-circuit potential), the terms of this competition are modified and may lead to the accumulation of corrosion products[20].

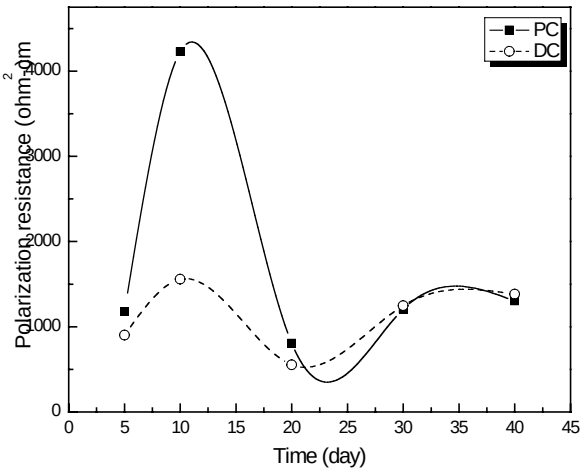

Figure 16: Polarization resistance with time calculated from the simulation of the high and low frequency responses of the impedance spectra for PC- and DC-deposited Zn-Sn.

The simulated sum of R_{film} and R_{ct} (Polarization resistance; R_p) are presented in Figure 16. Until 20 days of immersion, the R_p increased and then

decreased with time, which induced the formation and breakdown of Zn corrosion product. In this time period, the R_p of PC-deposited Zn-Sn shows higher values than that of DC-deposited Zn-Sn. However, after 20 days, the R_p for PC- and DC-deposited Zn-Sn showed similar values and stabilized due to the accumulation of Zn corrosion product on the surface. This result suggests that the grain refining effect does not guarantee a positive effect on the anticorrosive ability of Zn-Sn deposits after 30 days of immersion. Based on the above results, the EIS results are generally consistent with those evaluated by polarization tests, supporting the conclusion that PC-deposited Zn-Sn, with lower corrosion rate than DC-deposited Zn-Sn, should be the better anticorrosive coating in the initial stage of corrosion process for Zn dissolution.

Conclusions

- The formulation of a slightly acidic plating bath and deposition conditions for sacrificial Zn-Sn deposits containing 13~25 wt.% Sn were optimized.
- The Sn content in the deposit can be controlled by varying average current density, and as the average current density increase within the range 8~15 mA/cm^2, the Sn content in the deposit decreases less than 25 wt.%.
- The bath pH was optimized at a value of 5.7 based on the current efficiency and the deposit quality for the Zn-Sn deposition process.
- There was small composition difference between PC and DC deposition processes. However, at the same average current density, the grain size obtained in PC deposition being smaller than that in DC deposition, and more crystallized structure was obtained by PC deposition.
- In both cases of PC-, and DC-deposited Zn-Sn, the corrosion rate decreased with increasing Zn content in the deposit due to the formation of galvanic cells between Zn and Sn.
- The Zn-Sn prepared by PC deposition at 15 mA/cm^2 (87% Zn-13% Sn) exhibited better corrosion resistance than other Zn-Sn deposits owing to the more small grain size and crystallized structure. However, this behavior can be influenced on the anticorrosive ability of Zn-Sn deposits only in the initial stage of corrosion process.

Acknowledgments

Financial Support by AESF Research Contract, Project 107 and The Office of Naval Research under Grant No: N00014-04-1-0227 are gratefully acknowledged.

References

1. S. Swathirajan, *J. Electrochem. Soc.*, **133**, 671 (1986).
2. N.R. Short, S. Zhou & J.K. Bennis, *Surf. Coat. Technol.*, **79**, 218, (1996).
3. Y.P. Lin & J.R. Selman, *J. Electrochem. Soc.*, **140**, 1299, (1993).
4. C.C. Hu, C.K. Wang & G.L. Lee, *Electrochim. Acta*, **51**, 3692, (2006).
5. M.M. Abou-Krisha, *App. Surf. Sci.*, **252**, 1035, (2005).
6. O.A. Ashiru & J. Shirokoff, *App. Surf. Sci.*, **103**, 159, (1996).
7. St. Vitkova, V. Ivanova & G. Raichevsky, *Surf. Coat. Technol.*, **82**, 226, (1996).
8. C.J. Chen & C.C. Wan, *J. Electrochem. Soc.*, **136**, 2850, (1989).
9. A.M. Alfantazi & U. Erb, *Corrosion*, **52**, 880, (1996).
10. J.C. Puippe & F.H. Leaman, *Theory and Practice of Pulse Plating*, AESF Soc., 1986.
11. K. Lane, *J. Product Finish*, **42**, 22, (1989).
12. M.E. Warwick & P.E. Davis, *Plating Surf. Finish*, **74**, 77, (1987).
13. A. Bai & C.C. Hu, *Electrochim. Acta*, **47**, 3447, (2002).
14. A. Survila, Z. Mockus, R. Juskenas & V. Jasulaitiene, *J. Appl. Electrochem.*, **31**, 1109, (2001).
15. M. Pourbaix, *Atlas of Electrochemical Equilibria in Aqueous Solutions*, Permagon Press, New York, NY, 1966; p. 479.
16. E. Guaus & J. Torrent-Burgues, *J. Electroanal. Chem.*, **549**, 25, (2003).
17. H. Kim, N.P. Subramanian & B.N. Popov, *J. Power Sources*, **138**, 14, (2004).
18. N.S. Qu, D. Zhu, K.C. Chan & W.N. Lei, *Surf. Coat. Technol.*, **168**, 123, (2003).
19. Z.T. Park, Y.S. Choi, J.G. Kim and L. Chung, *Cement and Concrete Research*, **35**, 1814, (2005).
20. C. Cachet, F. Ganne, S. Joiret, G. Maurin, J. Petitjean, V. Vivier & R. Wiart, *Electrochim. Acta*, **47**, 3409, (2002).

